Thermogravimetric Investigations of Modified Iron Ore Pellets for Hydrogen Storage and Purification: The First Charge and Discharge Cycle

Viktor Hacker,[†] Rudolf Vallant,[‡] and Markus Thaler*,[†]

Institute for Chemistry and Technology of Inorganic Materials, CD-Laboratory for Fuel Cell Systems, Graz University of Technology, 8010 Graz, Austria, and Institute for Materials Science, Welding and Forming, Graz University of Technology, 8010 Graz, Austria

The reaction of iron with steam produces pure hydrogen, which can be directly used in polymer electrolyte fuel cells for power generation. Therefore iron, in its elemental form, can be used as a hydrogen storage and purification material. Besides thermodynamic properties, the hydrogen reception and release rate of the process are of special interest. To determine the reaction characteristics of iron contact mass for the first charging and discharging cycle, thermogravimetric analysis was used in the temperature range of 500−1000 °C. The influences of contact mass composition, reaction temperature, and gas composition on the redox reactions were determined. Contact masses with highly alkaline composition show faster reaction with steam at elevated temperatures. Acidic sample compositions accelerate the reduction with hydrogen at lower temperatures. The influence of hydrogen partial pressure and the suitability of methane, carbon monoxide, and synthesis gas for the contact mass reduction have been investigated intensely. Methane reduces the contact mass only at temperatures higher than 800 °C at an acceptable rate, but always leads to carbon deposition. Also, the operation with CO/H_2 mixtures results in carbon formation on the contact mass as soon as iron is present, whereby the rate of carbon production strongly depends on reaction temperature and gas composition. The product gas from steam reforming of methane is found to be a promising option as a reduction gas, leading to no carbon formation on the pellets at temperatures above 720 °C.

Introduction

Fuel cell technology has developed rapidly in recent years by increasing reliability and efficiency and decreasing production costs. Especially polymer electrolyte fuel cells (PEFC) are expected to be able to replace conventional combustion engines as an environmentally benign option for power generation. Because of its low tolerance against impurities like carbon monoxide, the fuel of choice for this kind of fuel cell is pure hydrogen.

Today most hydrogen is produced from hydrocarbons by steam reforming, autothermal reforming, or partial oxidation.[1] All these processes produce considerable amounts of CO as a byproduct, and several complex purification steps are needed to reach the desired hydrogen purity.

After purification, the hydrogen can be stored in compressed, liquid, or chemical form. Pressurized hydrogen tanks suffer from safety concerns,[2] and the compression of hydrogen consumes a considerable amount of energy. The liquefaction of hydrogen is very inefficient, and the boil-off leads to high losses.[3] Metal hydrides have a limited gravimetric storage density, and for most of the metal hydrides, the hydrogen release is an endothermic process for which heat must be supplied.

The sponge iron process[4,5] is able to accomplish the purification and storage of hydrogen in one single process by packing hot iron contact mass in a cartridge and water in a tank. For recharging, either the cartridge can be exchanged or the iron oxide can be reduced with a suitable reduction gas at refilling stations. Considering these aspects, the big advantage of this system is that only iron and water are to be stored, making this process a safe and efficient hydrogen storage and purification option.[6] As reported in ref 7, the thermochemical cycle can also be used for continuous gas purification in stationary applications by cyclic operation of two or more reactors in parallel.

In the storing process either hydrogen, CO, or gas mixtures such as synthesis gas are used to reduce iron oxide to elemental iron (eqs 1 and 2). This step is the so-called charging of the contact mass (Figure 1). Whenever energy is needed, steam is passed over the iron, and very pure hydrogen is released (eq 3, discharging of the contact mass).

reduction:

$$Fe_3O_4 + 4H_2 \rightarrow 3Fe + 4H_2O \qquad \Delta H°(800\ °C) = 97.7\ \text{kJ/mol (ref 8)} \quad (1)$$

$$Fe_3O_4 + 4CO \rightarrow 3Fe + 4CO_2 \qquad \Delta H°(800\ °C) = -13.5\ \text{kJ/mol (ref 8)} \quad (2)$$

oxidation:

$$3Fe + 4H_2O \rightarrow Fe_3O_4 + 4H_2 \qquad \Delta H°(800\ °C) = -97.7\ \text{kJ/mol (ref 8)} \quad (3)$$

According to the reaction in eq 3, the gravimetric storage density of the system is limited to a maximum of 4.8%. Especially for applications in forklifts or pallet lifting trucks, in which balance weight anyway is needed for stabilization, this system is seen as an attractive, low-cost hydrogen storage solution.

The steam−iron redox reactions are typical gas/solid reactions with relatively high activation energy and slow kinetics in both directions, especially at low temperatures. Otsuka et al.[9−11] investigated the influence of various metal additives on reaction kinetics and cycle stability. Urasaki et al.[12] modified iron with small amounts of palladium and zirconia to influence the properties for reduction and oxidation of the contact mass.

* To whom correspondence should be addressed. Tel.: +43 873 8784. Fax: +43 873 8782. E-mail: markus.thaler@tugraz.at.

[†] Institute for Chemistry and Technology of Inorganic Materials, CD-Laboratory for Fuel Cell Systems.

[‡] Institute for Materials Science, Welding and Forming.

10.1021/ie0616491 CCC: $37.00
Published on Web 11/28/2007

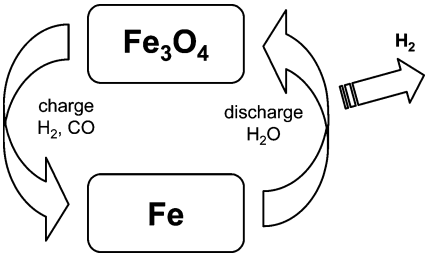

Figure 1. Principle of charging and discharging of the contact mass.

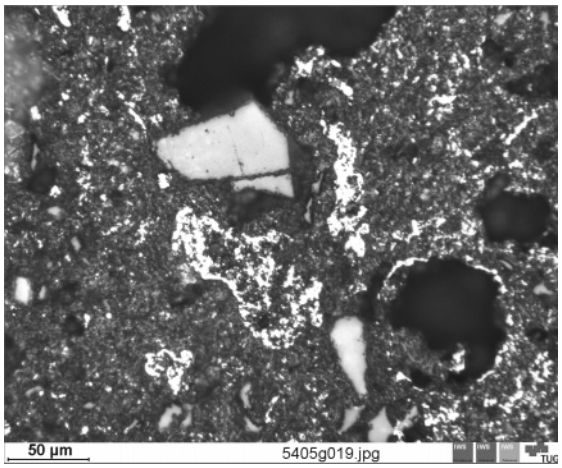

Figure 2. Cross section of a calcined pellet in an optical microscope.

Commercial iron ore pellets, used in the steel production industry, usually consist of Fe_2O_3, SiO_2, CaO, Al_2O_3, MgO, TiO_2, P_2O_5, and K_2O in different fractions. Eilers[13] observed a significant influence of the pellet composition from the different pellet suppliers in terms of reaction kinetics and cycle stability. It was reported that higher amounts of acidic additives such as SiO_2 and Al_2O_3 mitigate the sintering of the pellets over a number of cycles. Plzak et al.[14] reported that alkaline additives such as CaO decelerate the oxidation reaction at lower reaction temperatures.

Earlier investigations of our group concentrated on the role of SiO_2, CaO, and Al_2O_3 as sinter inhibitors. The results of porosity and structure analysis also showed higher cycle stability for highly acidic pellets.[15,16] In the present investigation, the effects of these additives during the first cycle are studied systematically in the temperature range of 500−900 °C using thermogravimetric analyses. The conversion−time curves of the reduction and the oxidation step give a clear view on the reaction run. This knowledge is essential for the design of the process in a larger scale system.[17] The effects of different gas compositions are pointed out, and the suitability of methane, CO, and synthesis gas as reducing agents are investigated.

Experimental Section

Iron ore pellets were formed on a rotating pelletizing plate at voestalpine Company (Linz/Austria) by mixing hematite Fe_2O_3 (85 mass %) with different amounts of additives and bentonite binder (approximately 1.5 mass %). Bentonite is mainly composed of SiO_2, Al_2O_3, MgO, and CaO. Therefore, in all samples traces of impurities can be found. The so-called green pellets, with a grain size fraction from 4 to 6.3 mm, were calcined at 1100 °C in air to increase the mechanical stability and to complete the oxidation of iron to hematite.

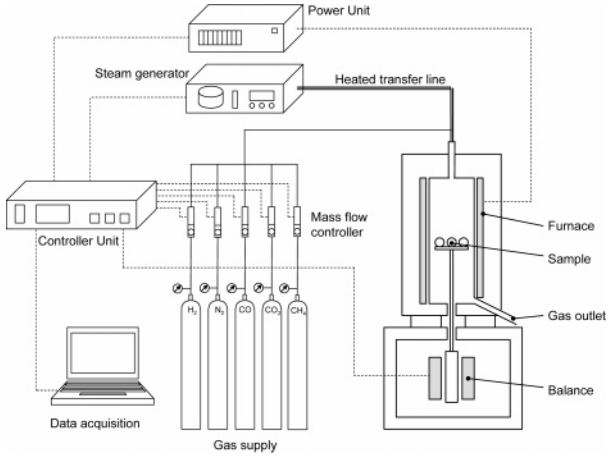

Figure 3. Setup of the thermogravimetric analysis system.

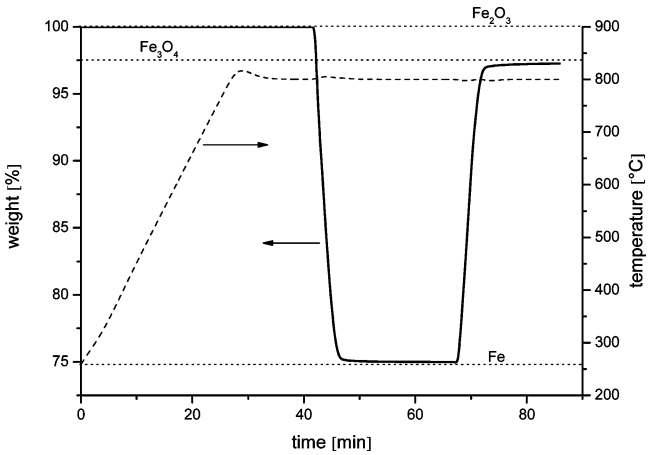

Figure 4. Weight change and temperature run during one cycle.

Table 1 provides the compositions of the pellet samples, the results of porosity measurements, and the alkalinity *A* of the calcined pellets investigated in this work.

The porosity of the pellets was measured using a mercury intrusion porosimeter (Thermofinnigan Pascal 140/440) with pressures up to 400 MPa. The initial porosity was in the range of 53−56% (for sample B, 41%). The alkalinity, *A*, of the pellets was calculated according to ref 18 by eq 4.

$$\text{alkalinity:}\quad A = \frac{\%\ \text{CaO} + \%\ \text{MgO}}{\%\ \text{SiO}_2 + \%\ \text{Al}_2\text{O}_3} \tag{4}$$

X-ray diffraction analysis (XRD) of the calcined pellets indicated that hematite (Fe_2O_3) was the main phase, i.e., the fully oxidized initial state. During the heat treatment, parts of the calcium formed a small amount of a new Ca−Fe phase ($Ca_2Fe_2O_5$), whereas Al_2O_3 and SiO_2 were found to remain stable in the pellets. The cross section of a calcined pellet in Figure 2 shows hematite as the main phase, bigger, sharp-edged SiO_2 crystals, and pores. The latter promote the access of the reactant gases.

Reduction and oxidation were performed by thermogravimetric analysis in a Netzsch STA 449 device, equipped with a special furnace to work under a steam atmosphere. A schematic illustration of the system setup is shown in Figure 3.

Five iron ore pellets with a diameter of about 4.5 mm and a total mass of 500 mg were heated in nitrogen atmosphere at a constant rate of 20 K/min to the desired reaction temperature.

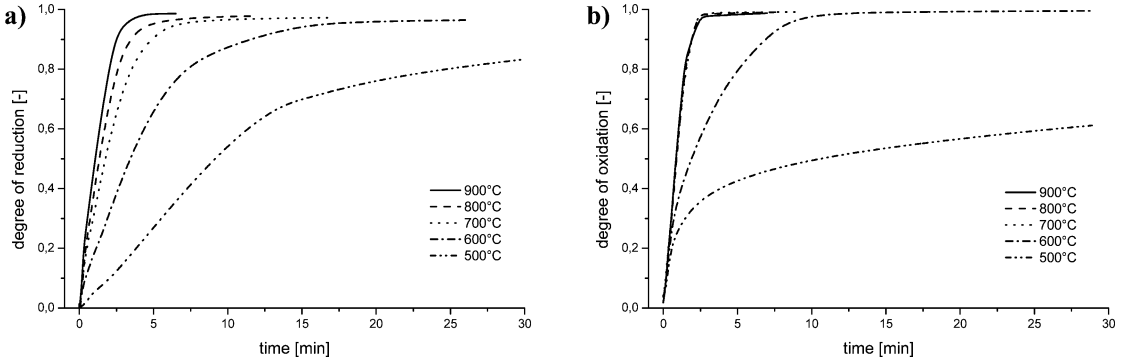

Figure 5. Degree of reactions for alkaline sample A with 10% CaO and 5% Al_2O_3 at different temperatures: (a) reduction H_2 = 250 mL/min, N_2 = 20 mL/min; (b) oxidation H_2O = 15 g/h, N_2 = 20 mL/min.

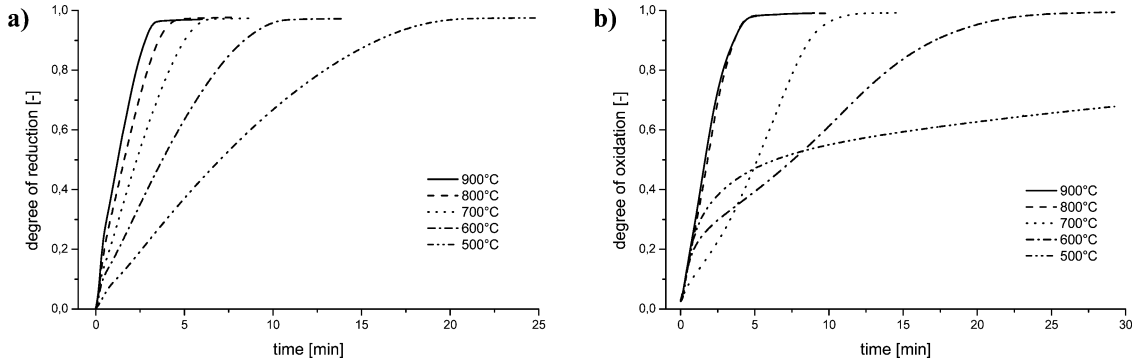

Figure 6. Degree of reactions for acidic sample E with 10% SiO_2 and 5% Al_2O_3 at different temperatures: (a) reduction H_2 = 250 mL/min, N_2 = 20 mL/min; (b) oxidation H_2O = 15 g/h, N_2 = 20 mL/min.

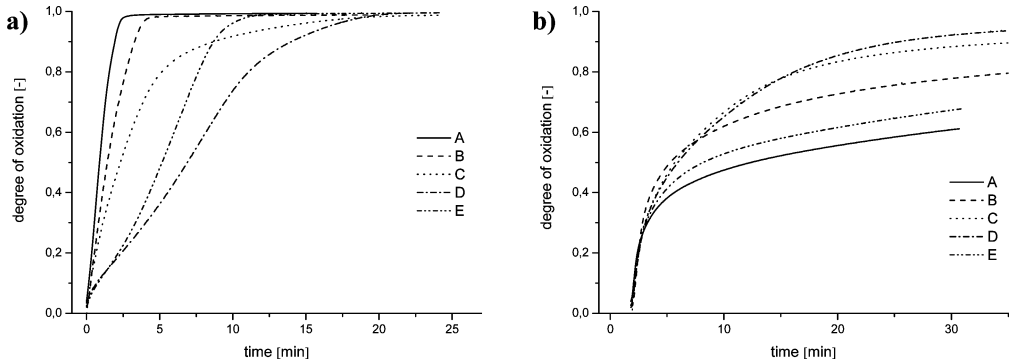

Figure 7. Degree of reaction for oxidation with steam, samples A−E: (a) at 700 °C and (b) at 500 °C.

Table 1. Compositional and Volumetric Characteristics of the Investigated Pellet Samples

sample	Fe_2O_2 [%]	SiO_2 [%]	CaO [%]	Al_2O_3 [%]	pore vol [mm^3/g]	surf. area [m^2/g]	av pore radius [nm]	porosity [%]	density [g/cm^3]	*A*
A	85	0	10	5	252.8	0.679	913.1	55.29	2.19	2.00
B	85	5	5	5	207.7	0.747	639.9	41.15	1.98	0.50
C	85	7.5	2.5	5	268.4	0.865	700.7	54.66	2.04	0.20
D	85	8.5	1.5	5	290.3	0.892	688.3	56.02	1.93	0.11
E	85	10	0	5	257.3	1.727	330.2	53.39	2.07	0.00

Then the sample was kept at constant temperature for 15 min followed by reduction in a gas stream of 250 mL/min reduction gas and 20 mL/min N_2. After the reduction of the sample was finished, i.e., no significant change of the weight was observed, the sample was oxidized with 15 g/h H_2O and 20 mL/min N_2. All experiments were carried out at ambient pressure.

Different research groups investigated the reduction of iron oxides with hydrogen[19,20] by using thermogravimetric analysis methods, but the oxidation reaction with steam was usually not addressed (except in ref 14). In this work, reduction with hydrogen, methane, carbon monoxide, and gas mixtures, as well as oxidation with steam, is discussed.

Results and Discussion

In Figure 4, the result of the thermogravimetric analysis of one redox cycle is shown. At the beginning of the experiment the sample consists of hematite with 15% additives. During the reduction, the hematite is completely reduced to sponge iron. The subsequent oxidation with steam proceeds to its thermo-

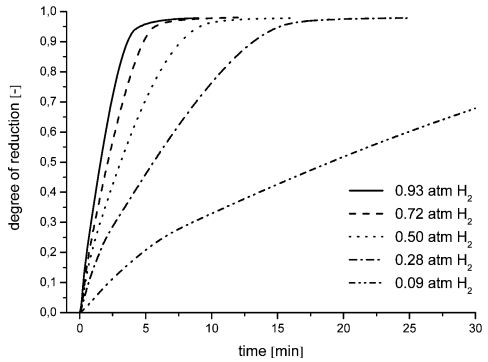

Figure 8. Degree of reaction for reduction with hydrogen at different partial pressures for sample D at 800 °C.

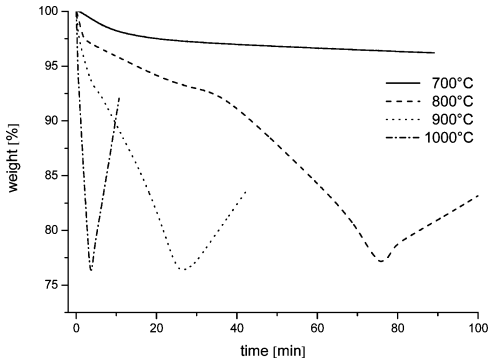

Figure 9. Weight loss during reduction with 250 mL/min CH_4 of sample D at temperatures from 700 to 1000 °C.

dynamic limit, the magnetite level (Fe_3O_4). Therefore, all the following charging and discharging steps are limited with the total reaction to iron and magnetite, respectively.

For the illustrations of the reaction runs, the degree of reaction, which is used in the figures below, is defined in eqs 5 and 6.

$$\text{degree of reduction:}\quad \mathrm{DR} = \frac{m_{\mathrm{Fe_2O_3}} - m(t)}{m_{\mathrm{Fe_2O_3}} - m_{\mathrm{Fe}}} \tag{5}$$

$$\text{degree of oxidation:}\quad \mathrm{DO} = \frac{m(t) - m_{\mathrm{Fe}}}{m_{\mathrm{Fe_3O_4}} - m_{\mathrm{Fe}}} \tag{6}$$

$m_{Fe_2O_3}$ is the initial sample mass, $m(t)$ is the sample mass at time t, m_{Fe} is the sample mass after complete reduction, and $m_{Fe_3O_4}$ is the sample mass after complete oxidation with steam.

Experiments with powdered samples at a temperature of 450 °C showed that additives mixed with iron oxide influenced the reaction rate significantly; e.g., additions of CaO decelerated the reaction at 450 °C, whereas additions of SiO_2 accelerated it. Investigations with the prepared pellet samples confirmed these results.

Reaction Characteristics for Alkaline Samples. At a temperature of 500 °C, the highly alkaline composition of sample A decelerates the reduction as well as the oxidation. The oxidation only proceeds quickly to a conversion rate of 30%. Then the reaction becomes slow, and within 30 min, only about 60% of the reaction is completed. On the other hand, the oxidation for sample A is accelerated at temperatures above 500 °C if compared to other samples of lower alkalinity under examination. In the temperature range from 700 to 900 °C, no difference in the oxidation reaction run can be detected for sample A (Figure 5.

Former investigations[15] of sample A showed that CaO promotes sintering of iron phases in periodic operation over a number of cycles. This effect is also supposed to be the reason for identical reaction runs at elevated temperatures (700−900 °C).

Reaction Characteristics for Acidic Samples. Pellets with lower alkalinity showed faster reaction at lower temperatures for the reduction stepas well as the oxidation step, if compared to sample A. In Figure 6, it can be seen that the oxidation reaction for sample E (alkalinity, $A = 0$) changes its character significantly at temperatures below 800 °C, indicating that rearrangements inside the pellets take place.

At 500 °C and a conversion rate of about 30%, the oxidation becomes slower and not more than 65% conversion degree is reached within 30 min. Also, this sample formulation shows

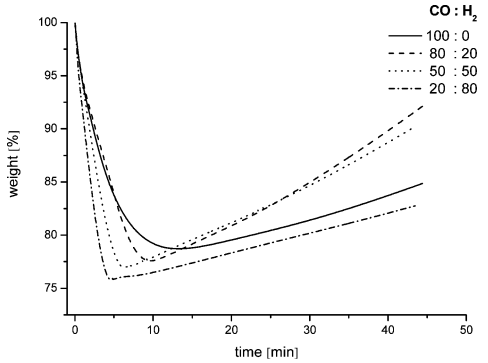

Figure 10. Weight loss during reduction with different CO/H_2 ratios of sample D at 800 °C.

nearly identical reaction characteristics at temperatures of 800 and 900 °C due to slight sintering during the reaction.

Influence of Pellet Composition. The influence of the sample composition on the reaction run differs with the applied temperature. Whereas for the reduction with hydrogen at temperatures higher than 600 °C no significant influence of the reaction temperature is detected, at lower temperatures sample A was reduced clearly the slowest, while other samples did not differ much. In contrast, the oxidation reaction with steam is influenced strongly by the sample composition over the whole temperature range under study. Higher alkalinity of the samples leads to faster reactions in the range of 600−900 °C. Figure 7a shows the influence of the pellet composition on the reaction run at 700 °C.

While sample A is already completely oxidized after 3 min, the acidic pellet composition of sample E needs almost 20 min for the full conversion into magnetite. In general, it can be concluded that pellets with higher alkalinity trend to react faster than acidic compositions.

At 700 °C, the reaction slopes of samples D and E show different shapes compared to the other samples investigated. The reaction starts very slowly and increases its rate after reaching 20% of full reaction degree. This behavior is found to be typical for alkalinity values lower than 0.2.

At 500 °C, in turn, sample A shows the poorest reaction rate, as seen in Figure 7b. However, no clear correlation between alkalinity and reaction rate can be found at this low temperature.

Generally, at lower temperatures, the oxidation is more limited than the reduction. Seiler and Emig[7] found out that this limitation is mainly defined by pore diffusion. While complete oxidation to magnetite at 900 °C only takes 5 min, at 600 °C, 25 min is needed. Limited by diffusion, the magnetite state is not reached at 500 °C within 30 min (Figure 6a).

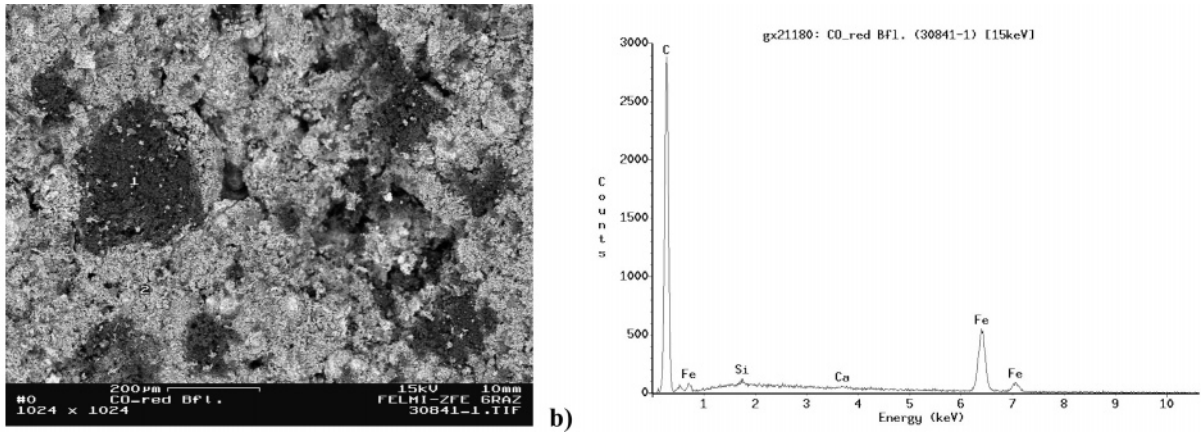

Figure 11. (a) SEM image of a CO reduced pellet (cross section); (b) EDX spot analysis of a dark area "1" in (a).

Influence of Hydrogen Partial Pressure. To determine the influence of different hydrogen/nitrogen partial pressures on the reaction rate, sample D (alkalinity 0.11) was reduced at 800 °C. As long as the hydrogen partial pressure is not less than 0.5 atm, the reaction is finished within 10 min (Figure 8).

The typical reaction curves, with a shoulder at about 10−12% degree of reduction, as reported by Pena et al.[20] for lower temperatures, cannot be observed here.

Among all reducing agents used for reduction in this study, hydrogen showed the fastest reaction for charging the contact mass. An additional advantage of using hydrogen is that the reduction can be completed at lower temperatures; e.g., the 100% DR charging at 500 °C takes 20 min. Consequently, by using hydrogen, the problem of carbon formation on the iron contact mass, which can occur with methane and CO, can be excluded.

Reduction with Methane. As described by different authors,[21−23] methane can also be used for reduction of iron oxide at high temperatures. The reduction of magnetite is highly endothermic and requires almost triple additional heating, compared to hydrogen (eq 7).

$$Fe_3O_4 + CH_4 \rightarrow 3Fe + 2H_2O + CO_2$$
$$\Delta H°(800\ °C) = 290.1\ \text{kJ/mol (ref 8)} \quad (7)$$

Experiments with pure methane for sample D show very slow reaction at 700 °C with only 5% weight loss of the iron oxide after 90 min. At 800 °C, the sample is almost totally reduced to sponge iron within 75 min. However, after the reduction is finished, carbon deposition takes place, as indicated by the subsequent increase in weight. The reduction rate with methane is only promising at temperatures higher than 900 °C, taking less than 25 min, but carbon formation still occurs (Figure 9).

Reduction with CO/H_2 Mixtures. The utilization of carbon monoxide as a reducing agent is of interest for commercial applications as biogas, coal gas, and synthesis gas always contain considerable amounts of CO. In the oxidation reaction with steam, pure hydrogen is produced as long as no carbon deposits on the contact mass during the previous reduction. The suitability of such gases for the reduction is tested on sample D with gas mixtures of different CO/H_2 ratios (Figure 10). Atmospheres with higher CO content lead to a slower reduction of the contact mass. In all these experiments, the weight increases after reaching a certain degree of reduction due to carbon deposition. Pure CO and mixtures of CO and H_2 always lead to carbon deposition on the pellets as soon as iron is present; see Figure 10.

Carbon Formation and Pellet Structure. Carbon formation is mainly described by the Boudouard equilibrium (eq 8). The reaction is strongly dependent on temperature and CO/CO_2 ratio in the reaction gas. Furthermore, iron is known to catalyze the formation of carbon.[24]

Boudouard equilibrium:

$$2CO \rightarrow CO_2 + C$$
$$\Delta H°(800\ °C) = -169.9\ \text{kJ/mol (ref 8)} \quad (8)$$

Scanning electron microsopic (SEM) images show that carbon is formed in clusters inside as well as on the surface of the pellet. Longer exposure of the sample in carbon-forming conditions leads to a tremendous loss in mechanical stability after just one cycle of operation. The interior structure is destroyed by the formation of carbon and cementite (Fe_3C). The energy-dispersive X-ray (EDX) analysis shows a high carbon peak in the dark areas of the SEM image, indicating high carbon concentration. In the surrounding brighter areas carbon can hardly be found and EDX analysis provides only the ingredients of the pellets; see Figure 11.

Long-time CO charging results in a carbon deposit of 3 mm thickness, enclosing the pellets. The carbon layer shows high specific volume and can be easily removed from the pellet surface. During the oxidation of carbon-coated pellets with steam, the carbon is oxidized first, and CO is produced according to eq 9. Not until most of the carbon has reacted does the iron start to oxidize.

$$C + H_2O \rightarrow CO + H_2$$
$$\Delta H°(800\ °C) = 135.8\ \text{kJ/mol (ref 8)} \quad (9)$$

In terms of mechanical stability and hydrogen quality, carbon formation must be avoided. Otherwise, due to the carbon gasification reaction during the oxidation with steam, undesired carbon monoxide is generated.

Reduction with Synthesis Gas. According to the Boudouard equilibrium (eq 8), carbon formation is favored at lower temperatures, while the addition of carbon dioxide to the reduction gas lowers the trend to carbon formation.

Therefore, a promising option for charging the contact mass is the use of synthesis gas. It can be produced by reforming of various hydrocarbons (fossil or renewable), which can be solid, liquid, or gaseous, and consists mainly of H_2, CO, CO_2, and H_2O in different ratios.

The typical dry gas composition of methane steam reforming (70% H_2, 20% CO, 10% CO_2) is used for the reduction of

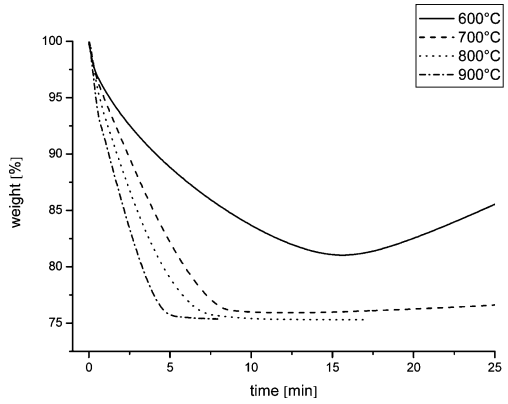

Figure 12. Weight loss during reduction with synthesis gas (70 H_2/20 CO/10 CO_2) of sample D for 600−900 °C.

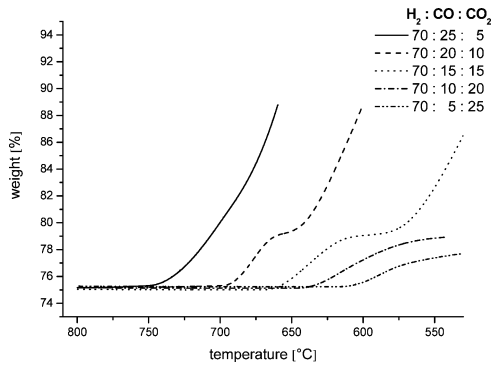

Figure 13. Carbon formation temperature for sample D charged with synthesis gas of different H_2/CO/CO_2 mixtures, determined by weight gain at constant cooling rate of 2 K/min.

sample D (Figure 12). Compared to the CO and CH_4 charging, carbon formation can be prevented at temperatures of 800 and 900 °C. Thereby a total conversion from hematite to iron is established. At 900 °C the sample is reduced quickly within 5 min. Also, for lower temperatures (700 °C), good results can be obtained, i.e., with little carbon formation after 8 min reduction time. Only partial reduction, followed by proceeding carbon formation, can be reached at 600 °C.

The formation of carbon is very constant after an initial period of time and proceeds faster at lower temperatures.

The critical carbon formation temperatures of different H_2/CO/CO_2 gas mixtures are determined as follows. First, sample D is reduced in the gas stream at 800 °C until the formation of sponge iron is completed. Then the temperature is lowered with a rate of 2 K/min. The weight of the sample remains constant until the temperature is reached at which carbon starts to deposit; see Figure 13. Hence, carbon deposition can be avoided by choosing a gas composition with higher CO_2 partial pressure or raising the reaction temperatures.

Summary and Conclusions

Modified iron ore pellets for hydrogen storage and purification were tested at different reducing and oxidizing conditions by thermogravimetric analysis. Especially the oxidation with steam was influenced by the pellet composition, while the influence on the reduction was small. High alkalinity of the pellets leads to higher reaction rates for oxidation at temperatures above 600 °C, whereas below this temperature the contrary effect was found. At higher temperatures, highly acidic pellet compositions took more than 2 times longer for complete oxidation.

Tests with different, carbon-containing, reduction agents led to undesirable carbon formation after the samples were reduced to sponge iron. Methane shows acceptable reduction rates at temperatures higher than 800 °C, but always leading to carbon deposition. In carbon monoxide containing reaction gases, carbon was formed with high CO contents, especially at temperatures below 800 °C.

Better results could be achieved by using gas mixtures containing CO_2. With a typical gas mixture of a methane steam reforming process, carbon deposition was excluded for reaction temperatures above 720 °C. This minimum temperature should be guaranteed in a reactor for a mixture of 70% H_2, 20% CO, and 10% CO_2 to avoid carbon formation during the charging of the storage system.

It is essential to avoid this carbon formation, as otherwise the pellets lose their mechanical stability and CO is produced during the oxidation reaction. In principle, methane and high CO containing gases can also be used as reduction gases as long as the reduction is stopped before iron is present in elemental form. The problem of cycle stability for charging and discharging of the contact mass with different gases is being intensely studied and will be published.

Acknowledgment

The authors appreciate the cooperation and support of the Austrian oil and gas company, OMV AG, and the Christian Doppler Society (CDG) for this project.

Literature Cited

(1) Momirlan, M.; Veziroglu, T. N. Current status of hydrogen energy, *Renewable Sustainable Energy Rev.* **2002**, *6*, 141.

(2) Utgikar, V. P.; Thiesen, T. Safety of compressed hydrogen fuel tanks: Leakage from stationary vehicles. *Technol. Soc.* **2005**, *27*, 315.

(3) Zhou, L. Progress and problems in hydrogen storage methods. *Renewable Sustainable Energy Rev.* **2005**, *9*, 395.

(4) Hacker, V. A novel process for stationary hydrogen production: the reformer sponge iron cycle (RESC). *J. Power Sources* **2003**, *118*, 311.

(5) Hacker, V.; Hierzer, J.; Evers, B. High efficient hydrogen production. Presented at the 15th World Hydrogen Conference. Yokohama, Japan, June 27−July 2, 2004.

(6) Otsuka, K.; Yamada, C.; Kaburagi, T. Hydrogen storage and production by redox of iron oxide for polymer electrolyte fuel cell vehicles. *Int. J. Hydrogen Energy* **2003**, *28*, 335.

(7) Seiler, H.; Emig, G. Reduction-oxidation cycles in a fixed-bed reactor with periodic flow reversal. *Chem. Eng. Technol.* **1998**, *21*, 6.

(8) Barin, I. *Thermochemical Data of Pure Substances Part I + II*; VCH Publishers: Weinheim, New York, 1989.

(9) Otsuka, K.; Kaburagi, T.; Yamada, C.; Takenaka, S. Chemical storage of hydrogen by modified iron oxides. *J. Power Sources* **2003**, *122*, 111.

(10) Takenaka, S.; Nomura, K.; Otsuka, K. Storage and formation of pure hydrogen mediated by the redox of modified iron oxides. *Appl. Catal., A: Gen.* **2005**, *282*, 333.

(11) Takenaka, S.; Kaburagi, T.; Otsuka, K. Storage and supply of hydrogen by means of the redox of the iron oxides modified with Mo and Rh species. *J. Catal.* **2004**, *228*, 66.

(12) Urasaki, K.; Tanimoto, N.; Matsukata, M. Hydrogen production via steam−iron reaction using iron oxide modified with very small amounts of palladium and zirconia. *Appl. Catal., A: Gen.* **2005**, *288*, 143.

(13) Eilers, A. Untersuchung handelsüblicher Eisenoxidpellets hinsichtlich ihrer Eignung für den Einsatz im Eisen-Wasserdampf-Wasserstoffsyntheseprozess. Diplomarbeit am Zentrum für Sonnenenergie- und Wasserstoffforschung Baden Württemberg, 1996, Ulm, Germany.

(14) Plzak, V.; Weinberger, M.; Garche, J. Investigations of the Kinetics and Catalysis of the Iron/Steam-Magnetite/Hydrogen-System in Low Temperature Regime with Regard of its Use to Produce and Store Hydrogen. *Hydrogen Energy Prog. XI* **1996**, *2*, 1175.

(15) Kindermann, H.; Kornberger, M.; Hacker, V. First investigations of structural changes of the contact mass in the RESC process for hydrogen production. *J. Power Sources* **2005**, *145*, 697.

(16) Thaler, M.; Hacker, V.; Anilkumar, M. Investigations of cycle behaviour of the contact mass in the RESC process for hydrogen production. *Int. J. Hydrogen Energy* **2006**, *31*, 2025.

(17) Hacker, V.; Faleschini, G.; Fuchs, H. Usage of biomass gas for fuel cells by SIR process. *J. Power Sources* **1998**, *71*, 226.

(18) Ivanov, O. Metallurgische Grundlagen zur Optimierung von Hochofenschlacken mit Bezug auf die Alkalikapazität. Dissertation an der Fakultät für Werkstoffwissenschaft und Werkstofftechnologie der Technischen Universität Bergakademie Freiberg, 2002, Freiberg, Germany.

(19) Pineau, A.; Kanari, N.; Gaballah, I. Kinetics of reduction of iron oxides by H_2 Part I: Low temperature reduction of hematite. *Thermochim. Acta* **2006**, *447*, 89.

(20) Pena, J. A.; Lorente, E.; Romero, E. Kinetic study of the redox process for storing hydrogen: Reduction stage. *Catal. Today* **2006**, *116*, 439.

(21) Galvita, V.; Sundmacher, K. Hydrogen production from methane by steam reforming in a periodically operated two-layer catalytic reactor. *Appl. Catal., A: Gen.* **2005**, *289*, 121.

(22) Otsuka, K.; Mito, A.; Takenaka, S. Production of hydrogen from methane without CO_2-emission mediated by indium oxide and iron oxide. *Int. J. Hydrogen Energy* **2001**, *26*, 191.

(23) Takenaka, S.; Hanaizumi, N.; Otsuka, K. Production of pure hydrogen from methane mediated by the redox of Ni- and Cr-added iron oxides. *J. Catal.* **2004**, *228*, 405.

(24) McCaldin, S.; Bououdina, M.; Grant, D. M. The effect of processing conditions on carbon nanostructures formed on an iron-based catalyst. *Carbon* **2006**, *44*, 2273.

Received for review December 21, 2006
Revised manuscript received September 14, 2007
Accepted October 1, 2007

IE0616491